

ON THE BENILOV-VYNNYCKY BLOW-UP PROBLEM

MARINA CHUGUNOVA

Institute of Mathematical Sciences
Claremont Graduate University
Claremont, CA 91711, USA

CHIU-YEN KAO ¹

Department of Mathematical Sciences
Claremont McKenna College
Claremont, CA 91711, USA

SARUN SEEPUN

Department of Mathematics
Pitzer College
Claremont, CA 91711, USA

(Communicated by Thomas P. Witelski)

ABSTRACT. We study an initial-boundary value problem for a fourth-order parabolic partial differential equation with an unknown velocity. The equation originated from the linearization of a two-dimensional Couette flow model, that was recently proposed by Benilov and Vynnycky. In the case of a 180° -contact angle between liquid and a moving plate Benilov and Vynnycky conjectured that the speed of the contact line blows up to infinity in finite time. In this paper we present numerical simulations and qualitative analysis of the model. We show that depending on the initial data and parameter values different long time behaviors of velocity can be observed. The speed of the contact line may blow up to infinity or converge to a constant.

1. Introduction. The contact line is the triple junction between solid, air and liquid flow. It is well known that Navier-Stokes equations with classical boundary conditions are not applicable if the free boundary of the flow intersects with a rigid boundary, resulting in the contact line. In 1980 Benney and Timson [3] analyzed the viscous liquid flow near the contact line and showed that, if the contact angle is 180° (the angle between the solid and the liquid interfaces), the contact line singularity, that is well known for the zero contact angle, does not arise and as a result the interface propagation is well-defined. Their local analysis did not include an asymptotic behavior of the contact line velocity. In a recently published paper, Benilov and Vynnycky [4], under an assumption of lubrication approximation regime, complemented the Benney and Timson results via asymptotic analysis of the global flow. Among other characteristics of the global flow they also determined the contact line velocity.

The Couette flow is represented schematically in Figure 1, where two parallel horizontal rigid plates are separated by the distance H . The upper plate is moving

2010 *Mathematics Subject Classification.* Primary: 76D08, 35K30; Secondary: 65M06.

Key words and phrases. Couette flow, contact angle, contact line singularity, blow-up, fourth-order parabolic equation.

¹This author's work is supported in part by NSF DMS 1318364.

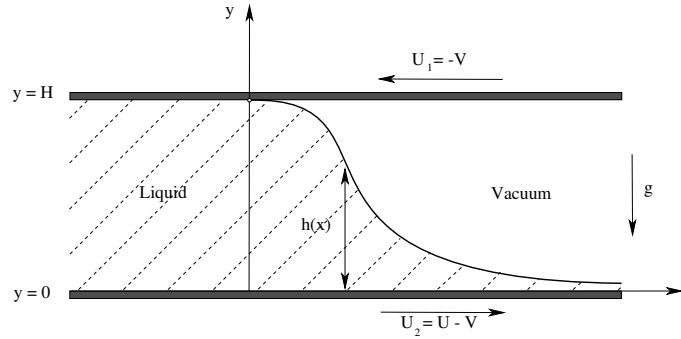


FIGURE 1. Couette flow with the free boundary, in the reference frame co-moving with the contact line.

to the left with a velocity U_1 and the lower plate is moving to the right with a velocity U_2 . The volume between these plates is filled with an incompressible viscous fluid on the left and with vacuum on the right, with the free boundary separation. The contact line is located on the upper plane and the position of the contact line in the reference frame that is co-moving with a contact line is fixed at the point $x = 0$. Under an assumption that a velocity of the upper plane matches a velocity of the lower plate relative to the upper plate. The time evolution of the profile of the liquid/vacuum free boundary is described by the graph of the function $h(x, t)$ for $x > 0$, and where h is the thickness of the liquid film.

We study the following initial-boundary value problem that was derived in [4, Eqs. (5.10), (5.15), (5.17) and (5.18)]:

$$\begin{cases} \tilde{h}_T + \frac{\alpha^3}{3} \tilde{h}_{XXXX} - v(T) \tilde{h}_X = 0, \\ \tilde{h}(X, 0) = \tilde{h}_0(X), \quad -1 \leq \tilde{h}_0(X) \leq 0, \\ \tilde{h}(0, T) = 0, \quad \tilde{h}_X(0, T) = 0, \quad \tilde{h}_{XXX}(0, T) = -\frac{3}{2\alpha^3}, \\ \lim_{X \rightarrow \infty} \tilde{h}_X(X, T) = \lim_{X \rightarrow \infty} \tilde{h}_{XXX}(X, T) = 0, \end{cases}$$

with two unknowns $\tilde{h}(X, T) = h(X, T) - 1$ and $v(T)$. In the original variable $h(X, T)$, the initial-boundary value problem is

$$\begin{cases} h_T + \frac{\alpha^3}{3} h_{XXXX} - v(T) h_X = 0, \\ h(X, 0) = h_0(X), \quad 0 \leq h_0(X) \leq 1, \\ h(0, T) = 1, \quad h_X(0, T) = 0, \quad h_{XXX}(0, T) = -\frac{3}{2\alpha^3}, \\ \lim_{X \rightarrow \infty} h_X(X, T) = \lim_{X \rightarrow \infty} h_{XXX}(X, T) = 0, \end{cases}$$

with two unknowns $h(X, T)$ and $v(T)$. With the scaling $x = \frac{3^{1/3}}{\alpha} X$ and $t = \frac{3^{1/3}}{\alpha} T$, we have

$$\begin{cases} h_t + h_{xxxx} - V(t) h_x = 0, \\ h(x, 0) = h_0(x), \quad 0 < h_0(x) \leq 1, \\ h(0, t) = 1, \quad h_x(0, t) = 0, \quad h_{xxx}(0, t) = -\frac{1}{2}, \\ \lim_{x \rightarrow \infty} h_x(x, t) = \lim_{x \rightarrow \infty} h_{xxx}(x, t) = 0. \end{cases}$$

In the special case when the contact line velocity was assumed to be a constant $V(t) = V_0$ the problem above was studied in [8]. The class of self-similar solutions for this partial differential equation (self-similar solutions do not satisfy the boundary conditions of the original problem) was constructed in [7].

Benilov, in personal communications, pointed out that a classical solution of the problem above (if it exists) should have an infinite number of constraints. It follows from the boundary conditions and from the partial differential equation that if a solution $h(x, t)$ is a classical one it should satisfy the condition $h_{xxxx}(0, t) = 0$. By differentiating this new condition with respect to t and by using the partial differential equation above as a substitution for h_t one obtains an infinite series of constraints (under an assumption of an infinite smoothness of the solution).

The existence of an infinite series of constraints for a solution of a partial differential equation is unusual, but this is not a unique case. A similar property has been noted for the so-called Ostrovsky equation for waves in a rotating ocean or in a channel with bottom topography [6, 2], as well as for Kadomtsev-Petviashvili equation [5, 1]. Finally, there are numerous models with a finite number of constraints, associated mostly with a scale of oceanic dynamics (see [10] and references therein). In all such cases, the constraints reflected an adjustment of the solution by fast dynamics, which were present in the original (exact) problem, but have been scaled out while deriving a slow-time asymptotic model. If the initial data taken does not comply with all the boundary constraints, it instantaneously evolves into a state satisfying all of them. However, since numerical methods cannot, generally, handle infinitely fast evolution, the adjusted state is not computed accurately. Once the adjustment is complete, the numerical solution begins to satisfy the equation accurately enough, but this adjustment makes the adjusted state different from the one originating from the initial condition given.

The structure of the article is as follows. In section two we prove non-existence of physically relevant stationary solutions in the Benilov-Vynnycky model and present analytical stationary solutions in non-physical regime. In the third section using energy method and functional inequalities we analyze a finite-interval approximation of the original problem. We derive estimates for $V(t)$ and for the existence times of solutions for different types of initial data. In section four we propose a simple numerical method, based on the finite difference approach, to solve the initial-boundary value problem of the Benilov-Vynnycky model. We show that depending on the initial data and parameter values, the magnitude of speed of the contact line may blow up to infinity or converge to a constant. The short discussion is presented in section five with a comparison of blow-up rates of numerical $V(t)$ with the logarithmic rate $V(t) \simeq c_1 \ln(t^* - t) + c_2$ predicted in [4] and with a power law rate $V(t) \simeq c_1 (t^* - t)^{-1/2} + c_2$ predicted recently in [9].

2. Formulation of the problem and analysis of stationary solutions. We consider the following initial-boundary value problem on \mathbb{R}^+ :

$$(P) \begin{cases} h_t + h_{xxxx} - V(t) h_x = 0, & (1a) \\ h(x, 0) = h_0(x), \quad 0 \leq h_0(x) \leq 1, & (1b) \\ h(0, t) = 1, \quad h_x(0, t) = 0, \quad h_{xxx}(0, t) = -\frac{1}{2}, & (1c) \\ \lim_{x \rightarrow \infty} h_x(x, t) = \lim_{x \rightarrow \infty} h_{xxx}(x, t) = 0, & (1d) \end{cases}$$

with two unknowns $h(x, t)$ and $V(t)$.

The solution $h(x, t)$ has a physical meaning only if $0 \leq h(x, t) \leq 1$ for $t \geq 0$ that implies $\lim_{x \rightarrow \infty} h(x, t) = h_\infty(t)$, $0 \leq h_\infty(t) \leq 1$.

The stationary solution of the problem above must satisfy

$$\begin{aligned}
 & \left\{ \begin{aligned} & u_{xxxx} - V u_x = 0, & (2a) \\ & u(0) = 1, \quad u_x(0) = 0, \quad u_{xxx}(0) = -\frac{1}{2}, & (2b) \\ & \lim_{x \rightarrow \infty} u_x(x) = \lim_{x \rightarrow \infty} u_{xxx}(x) = 0, & (2c) \end{aligned} \right. \quad (\text{Pstat})
 \end{aligned}$$

Theorem 2.1. *For $V > 0$, there exists a stationary solution to (Pstat) with $u(x) \geq 1$. Consequently, this stationary solution has no physical meaning.*

Proof. Integrating Equation (2a) over the interval $[0, x]$ and incorporating the first and third boundary conditions in (2b) give

$$u_{xxx} - Vu = -\frac{1}{2}(1 + 2V).$$

The general solution can be written as

$$u = c_1 e^{V^{1/3}x} + c_2 e^{-\frac{1}{2}V^{1/3}x} \cos\left(\frac{\sqrt{3}}{2}V^{1/3}x\right) + c_3 e^{-\frac{1}{2}V^{1/3}x} \sin\left(\frac{\sqrt{3}}{2}V^{1/3}x\right) + \frac{1 + 2V}{2V}. \quad (3)$$

From the condition $u(0) = 1$ it follows that

$$1 = c_1 + c_2 + \frac{1 + 2V}{2V}. \quad (4)$$

The condition $u_x(0) = 0$ provides that

$$0 = c_1 - \frac{1}{2}c_2 + c_3 \frac{\sqrt{3}}{2}. \quad (5)$$

If $V > 0$, the conditions $\lim_{x \rightarrow \infty} u_x(x) = \lim_{x \rightarrow \infty} u_{xxx}(x) = 0$ give $c_1 = 0$ and hence constants c_2 and c_3 are uniquely defined by the conditions (4) and (5) as

$$c_2 = -\frac{1}{2V} \text{ and } c_3 = \frac{1}{\sqrt{3}}c_2.$$

Notice that two boundary conditions at $x \rightarrow \infty$ lead to the same constraint and do not identify V uniquely. Furthermore, this solution has $\lim_{x \rightarrow \infty} u(x) = \frac{2V+1}{2V} > 1$ which is not physical. Two nonphysical stationary state solutions for $\lim_{x \rightarrow \infty} u(x) = 1.2$ and $\lim_{x \rightarrow \infty} u(x) = 1.5$ are shown in Figure 2 in the interval $[0, 20]$. □

It is worth mentioning that if $V < 0$, the conditions $\lim_{x \rightarrow \infty} u_x(x) = \lim_{x \rightarrow \infty} u_{xxx}(x) = 0$ give

$$c_2 = c_3 = 0.$$

This is in contradiction with the conditions (4, 5). Thus there is no physical stationary solution for this problem.

In the following section, we will study the problem above restricted to a finite interval. We will explore numerically how properties of solutions depend on the length of the truncated interval.

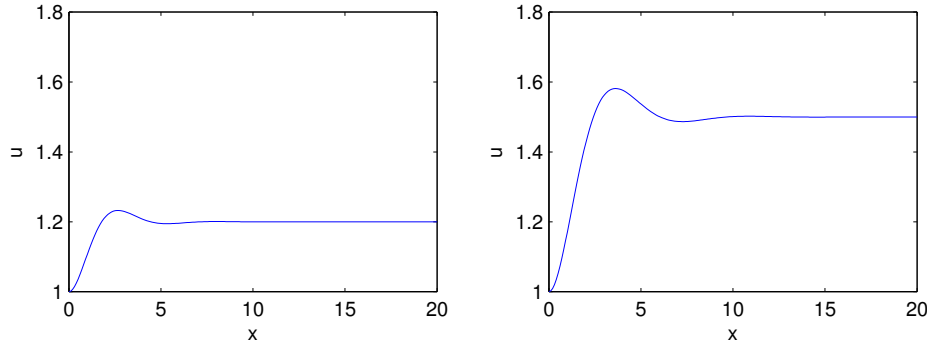


FIGURE 2. Two stationary state solutions with $\lim_{x \rightarrow \infty} u(x) = 1.2$ and $\lim_{x \rightarrow \infty} u(x) = 1.5$

3. Formulation of the finite-interval approximation and some qualitative analysis. We consider the following initial-boundary value problem on the finite interval $[0, L]$:

$$(P_{fin}) \begin{cases} h_t + h_{xxxx} - V(t) h_x = 0, & (6a) \\ h(x, 0) = h_0(x), \quad 0 \leq h_0(x) \leq 1, & (6b) \\ h(0, t) = 1, \quad h_x(0, t) = 0, \quad h_{xxx}(0, t) = -\frac{1}{2}, & (6c) \\ h_x(L, t) = h_{xxx}(L, t) = 0, & (6d) \end{cases}$$

with two unknowns $h(x, t)$ and $V(t)$.

Let us show that $V(t)$ can be positive only during a finite time interval provided that $0 \leq h \leq 1$.

Theorem 3.1. *If $0 \leq h(x, t) \leq 1$, $V(t)$ are classical solutions $h \in C^{4,1}$, $V \in C$ of the problem (P_{fin}) , and $V(t) \geq 0$ on $[0, T]$ then $T \leq \int_0^L h_0^2(x) dx$.*

Proof. Multiplying Equation (6a) by $h(x, t)$ and integrating over finite domain $(0, L)$, yields

$$\frac{d}{dt} \int_0^L h^2 dx + 2 \int_0^L h_{xx}^2 dx + 1 + V(t)(1 - h^2(L, t)) = 0. \tag{7}$$

Due to non-negativity of $V(t)$ and $1 - h^2(L, t)$ this implies that

$$\frac{d}{dt} \int_0^L h^2 dx \leq -1,$$

and integrating over $[0, T]$ we obtain the claimed upper bound for the time T . \square

Theorem 3.2. *If $0 \leq h(x, t) \leq 1$ and $V(t)$ are classical solutions $h \in C^{4,1}$, $V \in C$ of the problem (P_{fin}) and $V(t) \geq 0$ on $[0, T]$ then the total mass $M(t) = \int_0^L h(x, t) dx$ is decreasing.*

Proof. Integration of the equation over domain $(0, L)$, yields

$$\frac{d}{dt} \int_0^L h dx + \frac{1}{2} + V(t)(1 - h(L, t)) = 0. \tag{8}$$

This implies that $M'(t) < 0$ if $V(t) \geq 0$. \square

Similar if $V(t)$ is negative enough i.e $V(t) < -\frac{1}{2(1-h(L,t))}$ then the total mass is increasing.

Theorem 3.3. *If $h_{xx}(0, t) \leq 0$ and $0 \leq h(x, t) \leq 1$ is a classical solution $h \in C^{4,1}$ of the problem (P_{fin}) then the following inequality holds true*

$$1 - L^{1/2} \|h_{0,x}\|_2 e^{-(\pi/L)^4 t} \leq h(x, t) \leq 1 + L^{1/2} \|h_{0,x}\|_2 e^{-(\pi/L)^4 t}. \tag{9}$$

Proof. Multiplying Equation (6a) by h_{xx} and integrating over finite domain $[0, L]$, yields

$$\frac{1}{2} \frac{d}{dt} \int_0^L h_x^2 dx + \int_0^L h_{xxx}^2 dx = \frac{1}{2} h_{xx}(0, t).$$

As $x = 0$ is the attachment point of the liquid film to the upper moving plate that leads to the assumption that $h_{xx}(0, t) \leq 0$ and in this case we will obtain the energy dissipation

$$\frac{1}{2} \frac{d}{dt} \int_0^L h_x^2 dx + \int_0^L h_{xxx}^2 dx \leq 0. \tag{10}$$

If we apply the Poincare' inequality to the $h_x(x, t)$ with $h_x(0, t) = h_x(L, t) = 0$ and also to the $h_{xx}(x, t)$ with $\int_0^L h_{xx} dx = 0$ we will get

$$\int_0^L h_x^2 dx \leq \left(\frac{L}{\pi}\right)^2 \int_0^L h_{xx}^2 dx \leq \left(\frac{L}{\pi}\right)^4 \int_0^L h_{xxx}^2 dx. \tag{11}$$

It follows from (10, 11) that

$$\frac{1}{2} \frac{d}{dt} \int_0^L h_x^2 dx + \left(\frac{\pi}{L}\right)^4 \int_0^L h_{xx}^2 dx \leq 0. \tag{12}$$

This implies that

$$\int_0^L h_x^2 dx \leq e^{-2(\pi/L)^4 t} \int_0^L h_{0,x}^2 dx.$$

Using

$$\begin{aligned} |h(x, t) - h(0, t)| &= |h(x, t) - 1| = \left| \int_0^x h_x dx \right| \leq \\ &\leq L^{1/2} \left(\int_0^L h_x^2 dx \right)^{1/2} \leq L^{1/2} \|h_{0,x}\|_2 e^{-(\pi/L)^4 t}, \end{aligned}$$

we derive the upper and the low bounds for the thickness of the liquid film

$$1 - L^{1/2} \|h_{0,x}\|_2 e^{-(\pi/L)^4 t} \leq h(x, t) \leq 1 + L^{1/2} \|h_{0,x}\|_2 e^{-(\pi/L)^4 t}.$$

□

If the solution was global in time the bounds (9) in the theorem above would imply the uniform in time convergence toward $h = 1$. We can also use (9) to obtain the estimation of total mass:

$$L - L^{3/2} \|h_{0,x}\|_2 e^{-(\pi/L)^4 t} \leq M(t) \leq L + L^{3/2} \|h_{0,x}\|_2 e^{-(\pi/L)^4 t}.$$

The approach we used above is not straightforwardly applicable to the semi-infinite domain (P) due to the integrability problem. If we assume that a short-time initial dynamic is local in space and $\lim_{x \rightarrow \infty} h(x, t) = h_\infty$ (does not depend on time), then we can show that the contact line velocity $V(t)$ can be positive only during a finite time interval. Indeed, for any constant value of h_∞ we can introduce a new variable $\check{h} = h - h_\infty$. Due to the invariance of the partial differential equation, with

respect to the shift and scaling transformations, the boundary conditions can be preserved. We omit \check{h} -notations below.

Theorem 3.4. *If $0 \leq h(x, t) \leq 1$ and $V(t)$ are classical solutions $h \in C^{4,1}$, $V \in C$ of the problem (P) and $V(t) \geq 0$ on $[0, T]$ then $T \leq \int_0^\infty h_0^2(x) dx$.*

Proof. Multiplying Equation (1a) by $h(x, t)$ and integrating over domain $(0, +\infty)$, yield

$$\frac{d}{dt} \int_0^{+\infty} h^2 dx + 2 \int_0^{+\infty} h_{xx}^2 dx + 1 + V(t)(1 - h_\infty^2) = 0.$$

Due to non-negativity of $V(t)$ and $1 - h_\infty^2$ this implies that

$$\frac{d}{dt} \int_0^{+\infty} h^2 dx \leq -1,$$

and integrating over $[0, T]$ we obtain the claimed upper bound for the time T . \square

Theorem 3.5. *If $0 \leq h(x, t) \leq 1$ and $V(t)$ are classical solutions $h \in C^{4,1}$, $V \in C$ of the problem (P) and $V(t) \geq 0$ on $[0, T]$ then the total mass $M(t) = \int_0^{+\infty} h(x, t) dx$ is decreasing.*

Proof. Integrating the equation over domain $(0, +\infty)$, yields

$$\frac{d}{dt} \int_0^{+\infty} h dx + \frac{1}{2} + V(t)(1 - h_\infty) = 0.$$

This implies that $T \leq 2 \int_0^{+\infty} h_0 dx$ and $M'(t) < 0$ if $V(t) \geq 0$. \square

Similar if $V(t)$ is negative enough i.e $V(t) < -\frac{1}{2(1-h_\infty)}$ then the total mass is increasing.

Note that because

$$V(t) = -\frac{M'(t) + 1/2}{1 - h_\infty}, \tag{13}$$

a blow-up of $V(t)$ is possible only if there is a blow-up of the rate of change of the total mass or if $h_\infty = 1$.

Theorem 3.6. *There are countably many stationary solutions with $V > 0$ for the finite interval problem (P_{fin}).*

Proof. Denote $a = V^{\frac{1}{3}}$, the solution (2.8) can be written as

$$u = c_1 e^{ax} + c_2 e^{-\frac{1}{2}ax} \cos\left(\frac{\sqrt{3}}{2}ax\right) + c_3 e^{-\frac{1}{2}ax} \sin\left(\frac{\sqrt{3}}{2}ax\right) + \frac{1 + 2V}{2V}, \tag{14}$$

$$\begin{aligned} u_x &= c_1 a e^{ax} + a \left(-\frac{1}{2}c_2 + \frac{\sqrt{3}}{2}c_3\right) e^{-\frac{1}{2}ax} \cos\left(\frac{\sqrt{3}}{2}ax\right) \\ &+ a \left(-\frac{\sqrt{3}}{2}c_2 - \frac{1}{2}c_3\right) e^{-\frac{1}{2}ax} \sin\left(\frac{\sqrt{3}}{2}ax\right), \end{aligned}$$

$$\begin{aligned} u_{xx} &= c_1 a^2 e^{ax} + a^2 \left(-\frac{1}{2}c_2 - \frac{\sqrt{3}}{2}c_3\right) e^{-\frac{1}{2}ax} \cos\left(\frac{\sqrt{3}}{2}ax\right) \\ &+ a^2 \left(\frac{\sqrt{3}}{2}c_2 - \frac{1}{2}c_3\right) e^{-\frac{1}{2}ax} \sin\left(\frac{\sqrt{3}}{2}ax\right), \end{aligned}$$

$$u_{xxx} = c_1 a^3 e^{ax} + a^3 (c_2) e^{-\frac{1}{2}ax} \cos\left(\frac{\sqrt{3}}{2}ax\right) + a^3 (c_3) e^{-\frac{1}{2}ax} \sin\left(\frac{\sqrt{3}}{2}ax\right).$$

The boundary conditions $u_x(0) = 0$, $u_x(L) = 0$, and $u_{xxx}(L) = 0$ lead to

$$A \begin{pmatrix} c_1 \\ c_2 \\ c_3 \end{pmatrix} = \begin{pmatrix} 0 \\ 0 \\ 0 \end{pmatrix},$$

where

$$A = \begin{pmatrix} 1 & & & \\ e^{\frac{3}{2}\theta} & \left(-\frac{1}{2} \cos\left(\frac{\sqrt{3}}{2}\theta\right) - \frac{\sqrt{3}}{2} \sin\left(\frac{\sqrt{3}}{2}\theta\right)\right) & \left(\frac{\sqrt{3}}{2} \cos\left(\frac{\sqrt{3}}{2}\theta\right) - \frac{1}{2} \sin\left(\frac{\sqrt{3}}{2}\theta\right)\right) & \frac{\sqrt{3}}{2} \\ e^{\frac{3}{2}\theta} & \cos\left(\frac{\sqrt{3}}{2}\theta\right) & \sin\left(\frac{\sqrt{3}}{2}\theta\right) & \end{pmatrix}$$

and $\theta = aL$. The determinant of the matrix has to be zero in order to have nontrivial solutions, i.e.,

$$-\frac{\sqrt{3}}{2} + \left(\frac{3}{2} \sin\left(\frac{\sqrt{3}}{2}\theta\right) + \frac{\sqrt{3}}{2} \cos\left(\frac{\sqrt{3}}{2}\theta\right)\right) e^{\frac{3}{2}\theta} = 0$$

which implies that

$$\sqrt{3} \left(\sin\left(\frac{\sqrt{3}}{2}\theta + \frac{\pi}{6}\right) - \frac{1}{2} e^{-\frac{3}{2}\theta} \right) = 0.$$

Notice that $\theta = 0$ is a solution. Furthermore, since $f_1(\theta) = \sin\left(\frac{\sqrt{3}}{2}\theta + \frac{\pi}{6}\right)$ is an oscillatory function bounded above by 1 and bounded below by -1 and $f_2(\theta) = \frac{1}{2}e^{-\frac{3}{2}\theta}$ is a monotone decreasing function with range $[0, \frac{1}{2}]$, there are countably many solutions $\theta_n = LV_n^{1/3}$, $n = 1, 2, \dots$. See Figure 3. Let $(\tilde{c}_1, \tilde{c}_2, \tilde{c}_3)$ be a normalized vector that belongs to non-empty $Ker(A)$ then $(c_1, c_2, c_3) = \gamma(\tilde{c}_1, \tilde{c}_2, \tilde{c}_3)$, to define γ we need to use the boundary conditions $u(0) = 1$ and $u_{xxx}(0) = -\frac{1}{2}$ which give the constraints

$$\begin{aligned} u(0) &= c_1 + c_2 + \frac{1 + 2V}{2V} = 1, \\ u_{xxx}(0) &= a^3 (c_1 + c_2) = -\frac{1}{2}, \end{aligned}$$

which are equivalent to $c_1 + c_2 = -\frac{1}{2V}$. Hence $\gamma = -\frac{1}{2V(\tilde{c}_1 + \tilde{c}_2)}$. □

In Figure 4, we show the stationary solutions (14) for several choices of L with $\theta = \theta_1$ and several choices of θ with $L = 1$ respectively.

Theorem 3.7. *If u is the stationary solution of (P_{fin}) , h is the time-dependent solution of (P_{fin}) , and $\lim_{t \rightarrow \infty} V(t) = V_\infty$, we have $\lim_{t \rightarrow \infty} h(x, t) = u(x)$.*

Proof. In the finite interval $[0, L]$,

$$\begin{aligned} h_t + h_{xxxx} - V(t)h_x &= 0, \\ u_{xxxx} - V_\infty u_x &= 0. \end{aligned}$$

Let $w = h - u$. We have

$$w_t + w_{xxxx} - V(t)w_x + u_x(V_\infty - V(t)) = 0.$$

and

$$w(0, t) = 0, w_x(0, t) = 0, w_{xxx}(0, t) = 0,$$

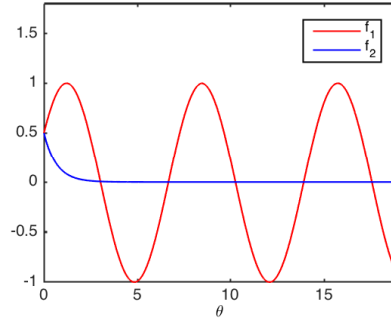


FIGURE 3. The solutions of $f_1(\theta) = f_2(\theta)$ where $f_1(\theta) = \sin\left(\frac{\sqrt{3}}{2}\theta + \frac{\pi}{6}\right)$ and $f_2(\theta) = \frac{1}{2}e^{-\frac{3}{2}\theta}$.

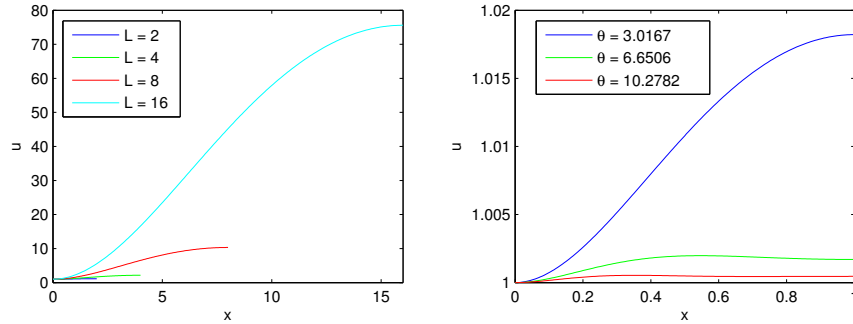


FIGURE 4. Left: The stationary solutions (14) for different L with $\theta = \theta_1$; Right: The stationary solutions (14) for different θ with $L = 1$.

$$w_x(L, t) = w_{xxx}(L, t) = 0.$$

Multiplying both sides by w_{xx} and then integrating from 0 to L , we obtain

$$\frac{d}{dt} \int_0^L \frac{1}{2}(w_x^2)dx + \int_0^L (w_{xxx})^2 dx = \int_0^L w_{xx}u_x (V_\infty - V(t)) dx.$$

By using Cauchy-Schwarz for the right hand side term and Poincare inequality for w_{xx} ,

$$\begin{aligned} \frac{d}{dt} \int_0^L \frac{1}{2}(w_x^2)dx + \int_0^L (w_{xxx})^2 dx &\leq \varepsilon^2 \int_0^L |w_{xx}|^2 dx + \frac{1}{\varepsilon^2} \int_0^L |u_x (V_\infty - V(t))|^2 dx \\ &\leq \left(\varepsilon \frac{L}{\pi}\right)^2 \int_0^L |w_{xxx}|^2 dx + \frac{1}{\varepsilon^2} \int_0^L |u_x (V_\infty - V(t))|^2 dx \end{aligned}$$

which gives

$$\frac{d}{dt} \int_0^L \frac{1}{2}(w_x^2)dx + \left(1 - \left(\varepsilon \frac{L}{\pi}\right)^2\right) \int_0^L (w_{xxx})^2 dx \leq \frac{1}{\varepsilon^2} \int_0^L |u_x (V_\infty - V(t))|^2 dx.$$

Since

$$u = -\frac{1}{2V_\infty} e^{-\frac{1}{2}V_\infty^{1/3}x} \cos\left(\frac{\sqrt{3}}{2}V_\infty^{1/3}x\right) - \frac{1}{\sqrt{3}} \frac{1}{2V_\infty} e^{-\frac{1}{2}V_\infty^{1/3}x} \sin\left(\frac{\sqrt{3}}{2}V_\infty^{1/3}x\right) + \frac{1+2V_\infty}{2V_\infty},$$

$$= -\frac{1}{\sqrt{3}V_\infty} e^{-\frac{1}{2}V_\infty^{1/3}x} \cos\left(\frac{\sqrt{3}}{2}V_\infty^{1/3}x - \frac{\pi}{6}\right) + \frac{1+2V_\infty}{2V_\infty},$$

Thus

$$|u_x| = \left| \frac{1}{\sqrt{3}} \frac{1}{V_\infty^{2/3}} e^{-\frac{1}{2}V_\infty^{1/3}x} \sin\left(\frac{\sqrt{3}}{2}V_\infty^{1/3}x\right) \right| \leq \frac{1}{2\sqrt{3}V_\infty^{2/3}}.$$

We then have

$$\frac{d}{dt} \int_0^L \frac{1}{2}(w_x^2)dx + \left(1 - \left(\frac{L}{\pi}\right)^2\right) \int_0^L (w_{xxx})^2 dx \leq \frac{1}{\varepsilon^2} \int_0^L |u_x (V_\infty - V(t))|^2 dx$$

$$\leq \frac{1}{\varepsilon^2} \frac{1}{12V_\infty^{4/3}} L |V_\infty - V(t)|^2.$$

Taking $\varepsilon < \frac{\pi}{L}$, we have $\lim_{t \rightarrow \infty} h(x, t) = u(x)$ when $\lim_{t \rightarrow \infty} V(t) = V_\infty$. □

4. Numerical method. In this section, we apply a semi-implicit method to study the solutions of the problem (P_{fin}). The computational domain is $(0, L)$. A uniform grid of points $x_j = j\Delta x$ where $0 \leq j \leq N$ and $N = \frac{L}{\Delta x}$ is used. The step size in time is Δt . The discretization of Eq. (6a) in time yields

$$\frac{h_j^{n+1} - h_j^n}{\Delta t} + (h_j^{n+1})_{xxxx} - V^{n+1}(h_j^n)_x = 0$$

where h_j^n is the numerical approximation of $h(x_j, t^n)$. The implicit discretization of h_{xxxx} is chosen to ensure that the step size can be chosen reasonably, i.e., $\Delta t \sim O(\Delta x)$ instead of $\Delta t \sim O(\Delta x)^4$. The explicit discretization of h_x is chosen to avoid nonlinearity in unknown variables h_j^{n+1} and V^{n+1} . Thus the updating formula is

$$(I + \Delta t D^4) h_j^{n+1} - V^{n+1} \Delta t D^1 h_j^n = h_j^n, \text{ for } j = 2, \dots, N - 2 \tag{15}$$

where I is the identity matrix and D^4, D^1 are numerical operators which approximate fourth-order and first-order differential operators respectively. We simply use the five-point central scheme for D^4 and the first order upwind scheme for D^1 which uses different discretization depends on the wind direction $-V$, i.e.,

$$D^4 h_j = \frac{h_{j+2} - 4h_{j+1} + 6h_j - 4h_{j-1} + h_{j-2}}{(\Delta x)^4},$$

and

$$D^1 h_j = \begin{cases} \frac{h_{j+1} - h_j}{\Delta x} & \text{if } V > 0, \\ \frac{h_j - h_{j-1}}{\Delta x} & \text{if } V < 0. \end{cases}$$

For the boundary conditions, we use the following discretization.

$$\begin{aligned} h(0, t) = 1 & \rightarrow h_0^n = 1, \\ h_x(0, t) = 0 & \rightarrow -3h_0^n + 4h_1^n - 1h_2^n = 0, \\ h_{xxx}(0, t) = -\frac{1}{2} & \rightarrow -\frac{5h_0^n + 18h_1^n - 24h_2^n + 14h_3^n - 3h_4^n}{2\Delta x^3} = \frac{1}{2}, \\ h_x(L, t) = 0 & \rightarrow h_{N-2}^n - 4h_{N-1}^n + 3h_N^n = 0, \\ h_{xxx}(L, t) = 0 & \rightarrow 5h_{N-4}^n - 18h_{N-3}^n + 24h_{N-2}^n - 14h_{N-1}^n + 3h_N^n = 0. \end{aligned} \tag{16}$$

The time step is chosen to satisfy the CFL condition $\Delta t \leq \Delta x/|V|$ and the number of interval N used is 128.

Notice that the initial velocity V^0 is not required when we solve (15) with the aforementioned boundary conditions. The discretized equation (15) and boundary conditions (16) form a linear system with $N + 2$ unknown h_j^{n+1} ($j = 0, \dots, N$), V^{n+1} , and $N + 2$ equations, which can be solved easily. The first step of calculation sometimes yields a large change in thickness h when the given initial data does not comply with all the boundary constraints. This is because the algorithm seeks the solution h and V to satisfy the equation and boundary conditions in one step. The contradiction between initial values and a partial differential equation was previously analyzed in [11, 12] and it is also imposed an additional difficulty on construction of a numerical solution of two-phase Stefan problem.

We first demonstrate the first order convergence of our numerical scheme with two initial conditions. The first initial condition is a 5-th order polynomial function which satisfies all the boundary conditions and $h(L) = 0.2$, i.e.,

$$h(x) = c_5x^5 + c_4x^4 + c_3x^3 + c_2x^2 + c_1x + c_0, \quad (17)$$

where

$$\begin{cases} c_0 = 1, \\ c_1 = 0, \\ c_2 = \frac{L^3 + 80h(L) - 80}{32L^2}, \\ c_3 = -\frac{1}{12}, \\ c_4 = \frac{7L^3 - 240h(L) + 240}{96L^4}, \\ c_5 = \frac{-L^3 + 48h(L) - 48}{48L^5} \end{cases}$$

with $L = 1$ while the second initial condition is $0.8 \cos^{10}(\frac{\pi}{2}x) + 0.2$ on the domain $[0, 1]$. We choose the second initial condition because it generates a wave front which looks like the one shown in [4]. Since the exact solution is not available, numerical tests were conducted on four different sizes of meshes: Δx , $2\Delta x$, $4\Delta x$ and $8\Delta x$ with $N = 256$. The step size $\Delta t = c\Delta x$ is chosen to satisfy the CFL constrain, i.e. $c < 1/|V|$. We choose $\Delta t = 5 \times 10^{-6}$ and $\Delta t = 1 \times 10^{-5}$ which are small enough for these two initial conditions, respectively. Denote the solution with mesh size Δx as $h_{\Delta x}$. We compute the differences between solutions in L_2 -norm for various times and list them in Table 1 and Table 2. For the polynomial initial condition, the blow-up time for the velocity V happened before $t = 0.02$ thus the value is not listed (In Table 1, we denote it as N/A). We use the notation order_1 (order_2) for the base-2 logarithm of ratio of consecutive differences between three solutions obtained by grid sizes Δx , $2\Delta x$, and $4\Delta x$ (by grid sizes $2\Delta x$, $4\Delta x$ and $8\Delta x$). It is clear that our scheme achieves the first order accuracy for both initial conditions at any given time which is away from the blow up time.

5. Numerical results.

5.1. Computational results for $h(L) = 0.2$. In Figure 5, we show the evolution of $h(x, t)$ and $V(t)$ with two different initial conditions (i) 5-th order polynomial which satisfies the boundary conditions and $h(L) = 0.2$ and (ii) $0.8 \cos^{10}(\frac{\pi}{2}x) + 0.2$ at different time. The time steps are chosen as 5×10^{-6} and 10^{-5} respectively and $\Delta x = 1/256$. The numerical solutions of $h(x, t)$ increase and get close to 1 no matter what the initial condition is. The velocity $V(t)$ approach to $-\infty$ when $h(x, t)$ approaches to 1. We terminated the numerical simulations when $V(t)$ becomes singular.

t	0.004	0.008	0.012
$\ h_{8\Delta x} - h_{4\Delta x}\ _2$	7.3330×10^{-3}	9.0178×10^{-3}	8.5428×10^{-3}
$\ h_{4\Delta x} - h_{2\Delta x}\ _2$	3.7293×10^{-3}	4.5260×10^{-3}	4.3535×10^{-3}
$\ h_{2\Delta x} - h_{\Delta x}\ _2$	1.8848×10^{-3}	2.2976×10^{-3}	2.1988×10^{-3}
order ₁	0.9755	0.9831	0.9725
order ₂	0.9845	0.9896	0.9854

t	0.016	0.02
$\ h_{8\Delta x} - h_{4\Delta x}\ _2$	7.4858×10^{-3}	N/A
$\ h_{4\Delta x} - h_{2\Delta x}\ _2$	3.8257×10^{-3}	3.8576×10^{-3}
$\ h_{2\Delta x} - h_{\Delta x}\ _2$	1.9347×10^{-3}	1.8337×10^{-3}
order ₁	0.9684	N/A
order ₂	0.9836	1.0729

TABLE 1. Accuracy test for the algorithm with the 5-th order polynomial initial condition which satisfies five boundary conditions and $h(1) = 0.2$.

t	0.004	0.008	0.012
$\ h_{8\Delta x} - h_{4\Delta x}\ _2$	5.3658×10^{-3}	8.2930×10^{-3}	8.3770×10^{-3}
$\ h_{4\Delta x} - h_{2\Delta x}\ _2$	2.8713×10^{-3}	4.2579×10^{-3}	4.3009×10^{-3}
$\ h_{2\Delta x} - h_{\Delta x}\ _2$	1.4475×10^{-3}	2.1356×10^{-3}	2.1650×10^{-3}
order ₁	0.9021	0.9618	0.9618
order ₂	0.9881	0.9955	0.9903

t	0.016	0.020
$\ h_{8\Delta x} - h_{4\Delta x}\ _2$	7.4567×10^{-3}	7.0468×10^{-3}
$\ h_{4\Delta x} - h_{2\Delta x}\ _2$	3.8448×10^{-3}	3.4685×10^{-3}
$\ h_{2\Delta x} - h_{\Delta x}\ _2$	1.9422×10^{-3}	1.7313×10^{-3}
order ₁	0.9556	1.0226
order ₂	0.9852	1.0025

TABLE 2. Accuracy test for the algorithm with the initial condition $0.8 \cos^{10}(\frac{\pi}{2}x) + 0.2$.

In Figure 6, we demonstrate how the evolution of $h(x, t)$ and $V(t)$ varies with respect to L with the initial condition as the 5-th order polynomial which satisfies the boundary conditions and $h(L) = 0.2$ for $L = 2$, and 6. We observe the finite-time blow up for $V(t)$ in both cases. For $L = 2$, $V(t)$ approaches $-\infty$ while, for $L = 6$, $V(t)$ approaches ∞ . Note that the initial condition for the case $L = 6$ is nonphysical. In Figure 7, we change the initial condition to $0.8 \cos^{10}(\frac{\pi}{2} \frac{x}{L}) + 0.2$. We see that the finite-time blow up for $V(t)$ decreases when L increases and both velocities approach ∞ . To understand the behavior of finite-time blow up solutions, it requires further theoretical analysis.

5.2. Computational results for $h(L) = 1.2$. In Figure 8, we start with non-physical initial condition as the 5-th order polynomial which satisfies the boundary conditions and $h(L) = 1.2$ for $L = 1, 5, 10$. When $L = 1$ and 5, the solutions h decrease and approach to stationary solutions (existence of which was obtained in

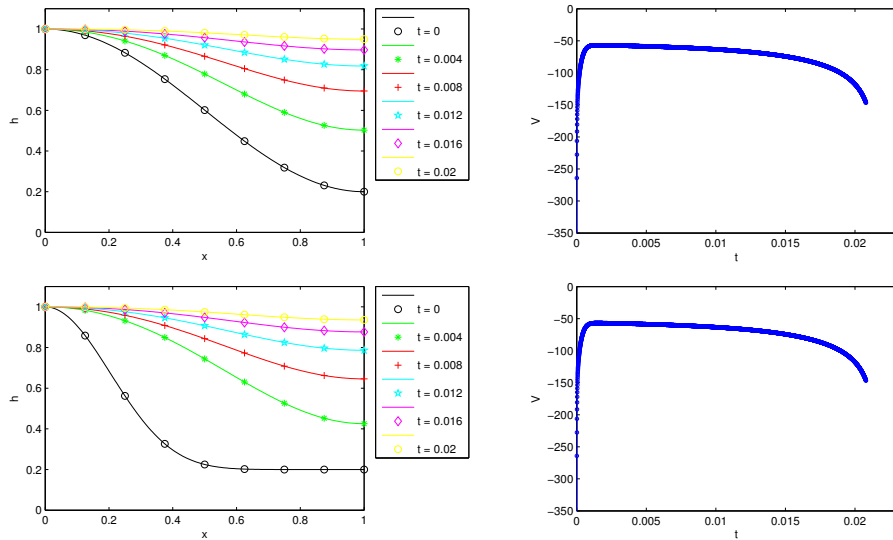


FIGURE 5. The evolution of $h(x, t)$ and $V(t)$ for two different initial conditions: (i) a 5-th order polynomial wave profile which satisfies the boundary conditions and (ii) $0.8 \cos^{10}(\frac{\pi}{2}x) + 0.2$.

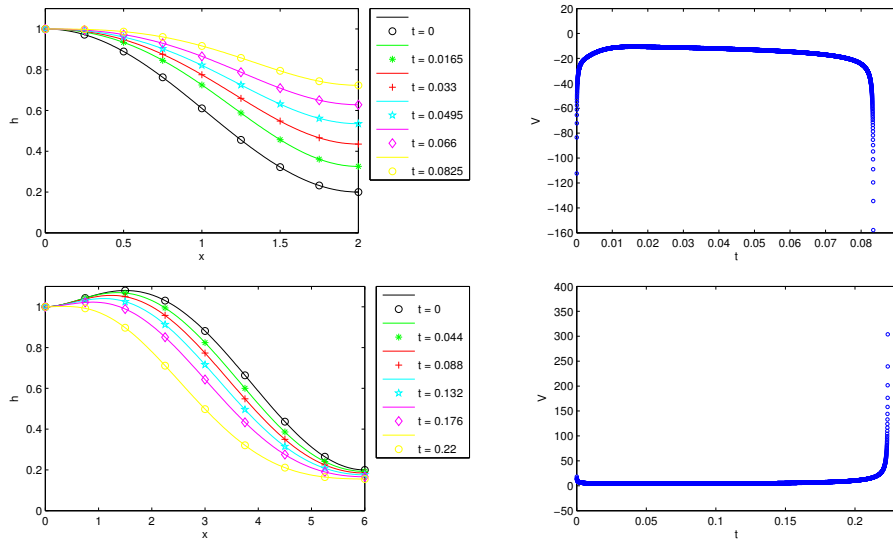


FIGURE 6. The evolution of $h(x, t)$ and $V(t)$ for the initial conditions given by a 5-th order polynomial (17) which satisfies the boundary conditions and $h(L) = 0.2$ for $L = 2$, and 6.

Theorem 3.6) while the velocities $V(t)$ approach to different constants. We observed that not all solutions are attracted to the stationary solutions. For $L = 10$, the velocity $V(t)$ blows up in finite time. In Figure 9, we start with nonphysical initial condition $0.8 \cos^{10}(\frac{\pi}{2} \frac{x}{L}) + 1.2$ for $L = 1, 5, 10$. When $L = 1$, the solution h

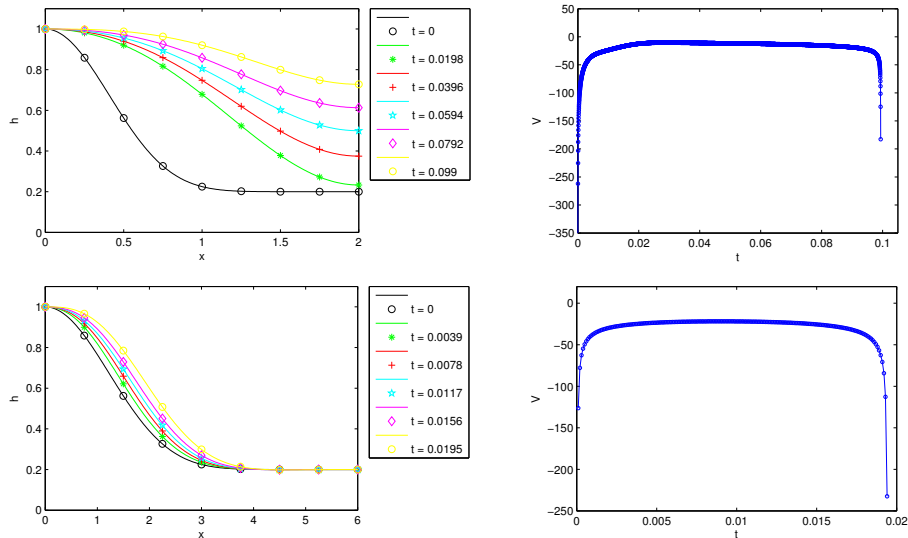


FIGURE 7. The evolution of $h(x, t)$ and $V(t)$ for two different L with the initial condition $0.8 \cos^{10}(\frac{\pi}{2} \frac{x}{L}) + 0.2$.

decreases and $V(t)$ increases first and approaches to a constant in time. For $L = 5$ and 10, the velocities $V(t)$ for both cases approach to a constant and the solution h remains bounded by 1 from below.

5.3. Comparison of solutions with various L . In Figure 10, we provide a comparison for solutions in the short ($L = 4$), medium ($L = 16$) and long ($L = 64$) intervals. As we discussed before, the first step of calculation sometimes yields a large change in the thickness h when the given initial data does not comply with all the boundary constraints. We thus compute the solution at $t = 10^{-3}$ with the initial condition $0.8 \cos^{10}(\frac{\pi}{2}x) + 0.2$ in the interval $[0, 1]$ and 0.2 for the rest of the interval $[1, 128]$ with the mesh size $\Delta x = 1/32$ (4097 grid points in total) and the time step $\Delta t = 10^{-5}$ first. Then we use part of this solution (the first 129, 513, and 2049 grid points) as the initial conditions for the intervals $L = 4, 16,$ and 64 . The evolution of $h(x, t)$ and $V(t)$ are shown in Figure 10 in the interval $[0, 6]$ since the solutions stay close to a constant after 6.

Notice that in the infinite interval, the boundary condition $\lim_{x \rightarrow \infty} h_x = 0$ implies $\lim_{x \rightarrow \infty} h_x x = 0$. However, this is not true for a finite interval truncated problem. Nevertheless, $h_x x(L, t)$ becomes closer to zero as L becomes large. The second order finite difference estimations give 3.27×10^{-4} , -1.05×10^{-11} and 2.18×10^{-14} for $L = 4, 16$ and 64 at $t = 0.0625$, respectively. We can see that the solutions h are very close to each other for different choices of L and the difference of V only becomes noticeable when the time is close to the blow up time. In Figure 11, we use the numerical results for $L = 64$ and do least-square fitting by using $V(t) \simeq c_1 \ln(t^* - t) + c_2$ [4] and $V(t) \simeq c_3 (t^* - t)^{-1/2} + c_4$ [9], respectively, for 800 grid points before the blow up time. With the choice $t^* = 0.064563$, the best fittings are $V(t) \simeq 15.14 \ln(t^* - t) + 61.54$ denoted by blue line and $V(t) \simeq -0.5459 \ln(t^* - t) - 14.51$ denoted by green line, respectively. We see that the blow up rate of the contact line velocity $V(t)$ is between the logarithmic one proposed in [4] and the power law one in [9].

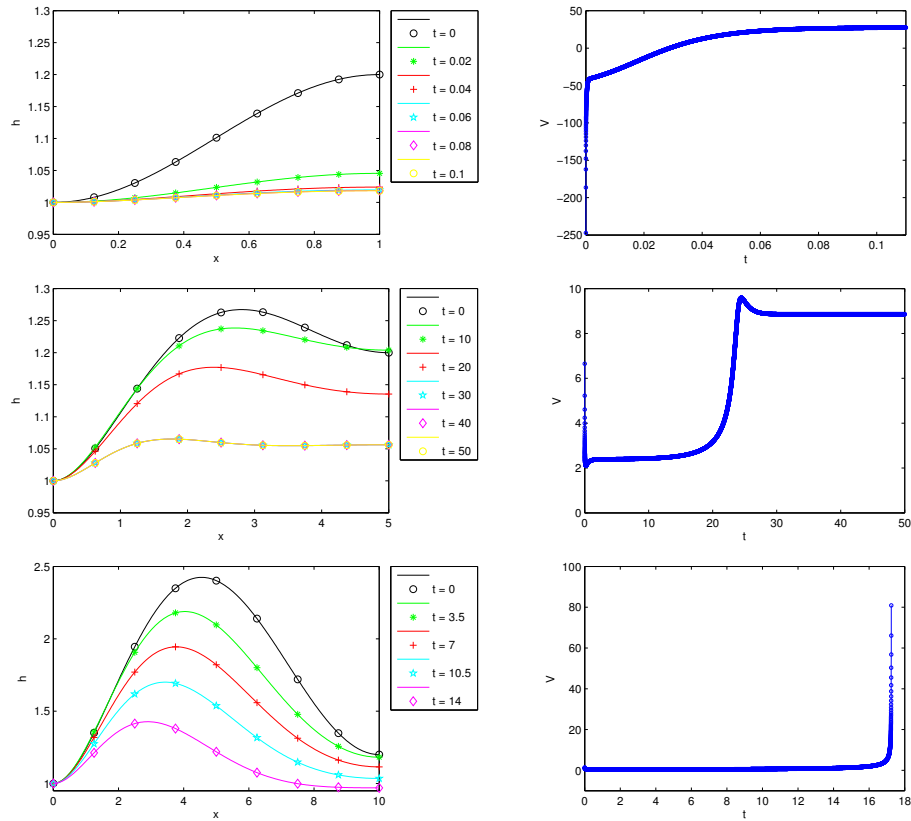


FIGURE 8. The evolution of $h(x,t)$ and $V(t)$ for the initial conditions given by a 5-th order polynomial (17) which satisfies the boundary conditions and $h(L) = 1.2$ for $L = 1, 5$, and 10 .

From the above simulations, we observe that $|V|$ blows up in finite time for physical initial conditions while V may blow up in finite time or stay bounded for nonphysical initial conditions.

6. Discussion. We have thus explored the behavior of viscous liquid film between two parallel horizontal moving plates. In particular, we showed analytically and numerically that the contact line velocity $V(t)$ exhibits a finite time singularity if the contact angle is 180° . We have also estimated the local existence times of solutions for the related model (1a) and studied stationary solutions.

First, it is suggested by the results shown in Figure 11 that the blow up rate of the contact line velocity $V(t)$ is between the logarithmic one proposed in [4] and the power law one in [9]. Rigorous asymptotical analysis of the blow-up rate of $V(t)$ is not straightforward and is open for future study. Second, in non-physical regime the steady state seems to be an attractor but we were able to prove this only under additional assumptions. Finally, one can develop more accurate numerical computations to better resolve the singular behavior of $V(t)$.

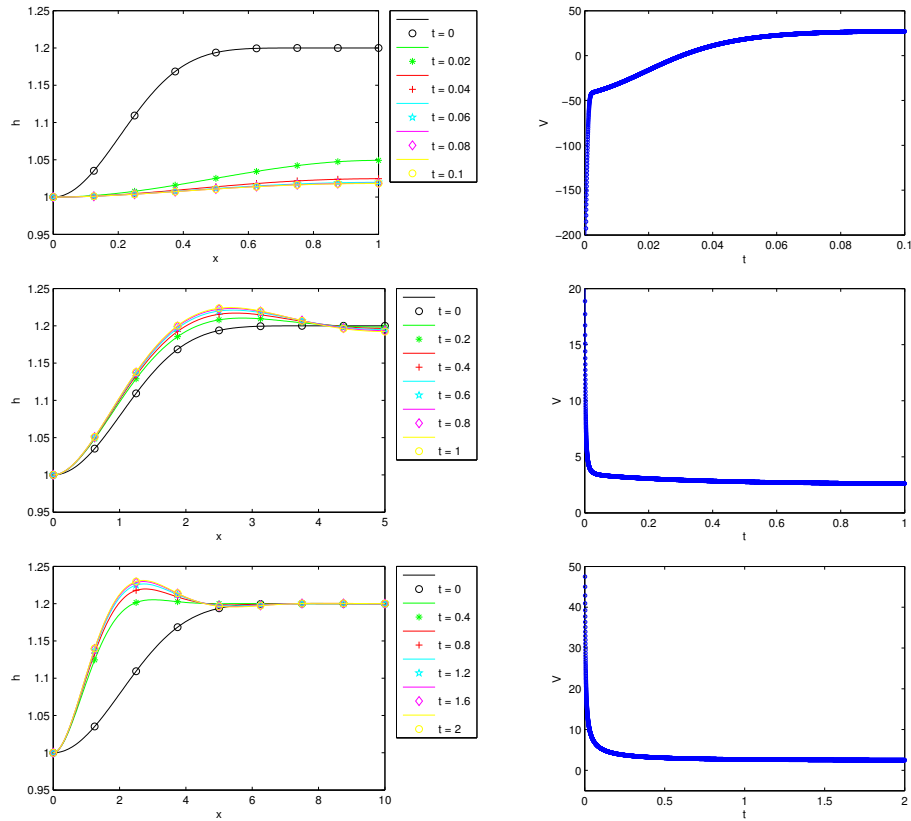


FIGURE 9. The evolution of $h(x, t)$ and $V(t)$ for the different initial conditions: $0.8 \cos^{10}(\frac{\pi x}{2L}) + 1.2$ for $L = 1, 5, 10$.

Acknowledgments. The authors would like to thank the referee for the thorough review and very useful comments. This work was partially supported by a grant from the Simons Foundation (#275088 to Marina Chugunova).

REFERENCES

- [1] M. J. Ablowitz and J. Villarroel, On the Kadomtsev-Petviashvili equation and associated constraints, *Stud. Appl. Math.*, **85** (1991), 195–213.
- [2] E. S. Benilov, On the surface waves in a shallow channel with an uneven bottom, *Stud. Appl. Math.*, **87** (1992), 1–14.
- [3] D. J. Benney and W. J. Timson, The rolling motion of a viscous fluid on and off a rigid surface, *Stud. Appl. Math.*, **63** (1980), 93–98.
- [4] E. S. Benilov and M. Vynnycky, Contact lines with a 180° contact angle, *J. Fluid Mech.*, **718** (2013), 481–506.
- [5] B. B. Kadomtsev and V. I. Petviashvili, On the stability of solitary waves in weakly dispersing media, *Sov. Phys. Dokl.*, **15** (1970), 539–541.
- [6] L. A. Ostrovskii, Nonlinear internal waves in the rotating ocean, *Okeanologiya*, **18** (1978), 181–191.
- [7] D. E. Pelinovsky and A. R. Giniyatullin, Finite-time singularities in the dynamical evolution of contact lines, *Bulletin of the Moscow State Regional University (Physics and Mathematics)*, **3** (2013), 14–24.

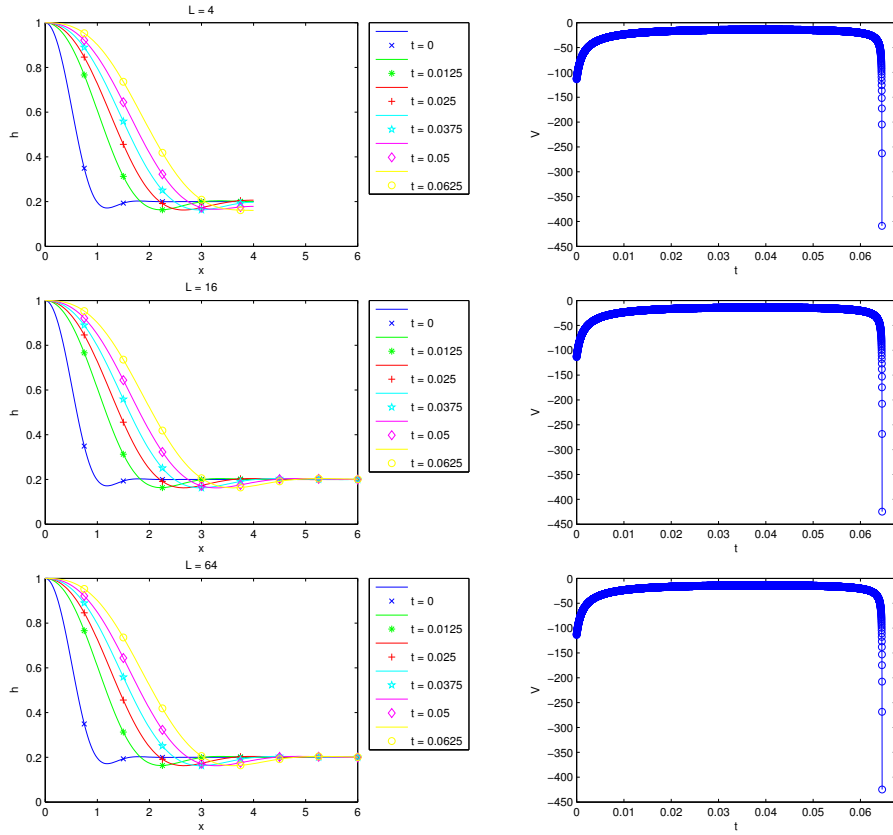


FIGURE 10. The evolution of $h(x, t)$ and $V(t)$ for $L = 4, 16,$ and 64 .

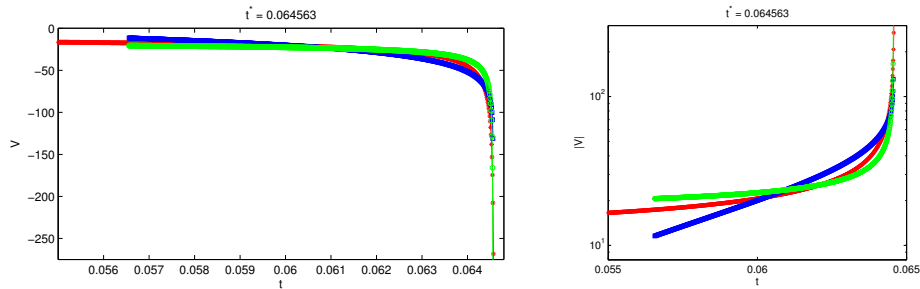


FIGURE 11. Left: the red line corresponds to the numerical contact line velocity $V(t)$, the blue line is the least-square fitting of the numerical data for $V(t)$ using $V(t) \simeq c_1 \ln(t^* - t) + c_2$ and the green line is the least-square fitting using $V(t) \simeq c_3 (t^* - t)^{-1/2} + c_4$. Right: the semilogy plot to see different fittings more clearly.

[8] D. E. Pelinovsky, A. R. Giniyatullin and Y. A. Panfilova, On solutions of the reduced model for the dynamical evolution of contact lines, *Transactions of Nizhni Novgorod State Technical University n.a. Alexeev N.4*, **94** (2012), 45–60.

- [9] D. E. Pelinovsky and C. Xu, On numerical modelling and the blow-up behavior of contact lines with a 180° contact angle, *J. Engineer. Math.*, 2015.
- [10] J. Le Sommer, G. M. Reznik and V. Zeitlin, [Nonlinear geostrophic adjustment of long-wave disturbances in the shallow-water model on the equatorial beta-plane](#), *Journal of Fluid Mechanics*, **515** (2004), 135–170.
- [11] M. Vynnycky and S. L. Mitchell, [On the accuracy of a finite-difference method for parabolic partial differential equations with discontinuous boundary conditions](#), *Num. Heat Trans B*, **64** (2013), 275–292.
- [12] S. L. Mitchell and M. Vynnycky, [On the numerical solution of two-phase Stefan problems with heat-flux boundary conditions](#), *J. Comp. Appl. Maths*, **264** (2014), 49–64.

Received July 2013; 1st revision December 2013; final revision June 2014.

E-mail address: Marina.Chugunova@cgu.edu

E-mail address: Ckao@cmc.edu

E-mail address: sseepun@students.pitzer.edu